



**HAL**  
open science

## Opti-Morph, a new platform for sandy beach dynamics by constrained wave energy minimization

Megan Cook, Frédéric Bouchette, Bijan Mohammadi, Samuel Meulé, Nicolas  
Fraysse

► **To cite this version:**

Megan Cook, Frédéric Bouchette, Bijan Mohammadi, Samuel Meulé, Nicolas Fraysse. Opti-Morph, a new platform for sandy beach dynamics by constrained wave energy minimization. 2021. hal-03272051v1

**HAL Id: hal-03272051**

**<https://hal.science/hal-03272051v1>**

Preprint submitted on 28 Jun 2021 (v1), last revised 13 Mar 2023 (v4)

**HAL** is a multi-disciplinary open access archive for the deposit and dissemination of scientific research documents, whether they are published or not. The documents may come from teaching and research institutions in France or abroad, or from public or private research centers.

L'archive ouverte pluridisciplinaire **HAL**, est destinée au dépôt et à la diffusion de documents scientifiques de niveau recherche, publiés ou non, émanant des établissements d'enseignement et de recherche français ou étrangers, des laboratoires publics ou privés.

# Opti-Morph, a new platform for sandy beach dynamics by constrained wave energy minimization

Megan Cook<sup>1,3,5</sup>, Frédéric Bouchette<sup>1,3</sup>, Bijan Mohammadi<sup>2,3</sup>, Samuel Meulé<sup>3,4</sup>, Nicolas Fraysse<sup>5</sup>

<sup>1</sup>GEOSCIENCES-M, Univ Montpellier, CNRS, Montpellier, France

<sup>2</sup>IMAG, Univ Montpellier, CNRS, Montpellier, France

<sup>3</sup>GLADYS, Univ Montpellier, CNRS, Le Grau du Roi, France

<sup>4</sup>CEREGE, Univ Montpellier, CNRS, MHN, Aix-en-Provence, France

<sup>5</sup>BRL Ingénierie, Nîmes, France

## Key Points:

- A new coastal dynamics morphodynamic model is introduced also accounting for the evolution of the shoreline
- The model automatically adapts to either basin or open sea settings and only requires two hyper-parameters (the sand abrasion and the critical angle of repose)
- Opti-Morph is compared to wave-flume experimental data and XBeach numerical simulations

## Abstract

This paper focuses on a new approach to describe coastal morphodynamics, based on optimization theory, and more specifically on the assumption that a sandy seabed evolves in order to minimize a wave-related function, the choice of which depends on what is considered the driving force behind coastal morphodynamics. The numerical model derived from this theory uses a gradient descent method and permits to account for physical constraints such as sand conservation in basin experiments. Hence, the model automatically adapts to either basin or open sea settings and only involves two hyper-parameters: the sand abrasion and the critical angle of repose. The model behavior is illustrated on a flume configuration. Comparison of the resulting seabed with experimental data as well as with the results of the widely distributed coastal morphodynamic software XBeach demonstrate the potential of a model by wave energy minimization.

## 1 Introduction

Optimization theory is the study of the evolution of a system, while searching systematically for the minimum of a function derived from physical properties of the system. In this paper, we have applied this approach to coastal dynamics, with our primary objective to simulate the interactions between the waves and seabed. Continuing the work of (Mohammadi & Bouharguane, 2011) and (Mohammadi & Bouchette, 2014), we have developed a theory and designed a model that describes the evolution of the seabed while taking into account the coupling between morphodynamic and hydrodynamic processes. This study focuses on a theoretical and numerical approach to the modeling of this coupling, based on the assumption that the seabed adapts to minimize a certain wave-related function. The choice of this function determines the driving force behind the morphological evolution of the seabed. This optimization problem is subjected to a certain number of constraints, allowing for a more accurate description of the morphodynamic evolution.

This study is accompanied by the development of a numerical hydro-morphodynamic model, which has the advantages of being fast, robust and of low complexity. The model was given the name "Opti-Morph".

With the purpose of validating Opti-Morph, we compare the results of the numerical simulation with that of another numerical morphodynamic model. We choose XBeach (Roelvink et al., 2009). Originally designed to simulate the impact of extreme storms on beaches, XBeach is considered a reputable model in the coastal dynamic community (Bugajny, Furmanczyk, Dudzinska-Nowak, & Papliska-Swerpel, 2013; Williams, Esteves, & Rochford, 2015; Zimmermann et al., 2012).

The paper starts with a description of the hydrodynamic model, based on linear theory and the morphodynamic model (Opti-Morph) based on wave-energy minimization. A comparison is then conducted between the results of the numerical simulation with the experimental data, as well as the results produced by the XBeach morphodynamic module.

### 1.1 State of the Art

Numerical models of morphodynamic processes are seen as a valuable tool for understanding and predicting the evolution of the sediment over time in coastal areas. Various methods have been developed over the last forty years and vary in degrees of complexity.

Different morphodynamic models exist in the literature, ranging from empirical models (de Vriend, Bakker, & Bilsse, 1994; Gravens, 1997; Kana, Hayter, & Work,

1999; Ruessink & Terwindt, 2000) to process-based models. The latter can be sorted into several categories, such as profile evolution models (Larson & Kraus, 1989; Larson, Kraus, & Byrnes, 1990; Nairn & Southgate, 1993), computed using only cross-shore transport, 2D morphological models (Coeffe & Pechon, 1982; Fleming & Hunt, 1977; Johnson, Brker, & Zyserman, 1995; Latteux, 1980; Maruyama & Takagi, 1988; Nicholson et al., 1997; Roelvink et al., 2009; Wang, Miao, & Lin, 1993; Watanabe, Maruyama, Shimizu, & Sakakiyama, 1986; Yamaguchi & Nishioka, 1985) which use depth-averaged wave and current equations to model the sediment transport, while neglecting the vertical variations of waves and current, as well as 3D and quasi-3D models (Briand & Kamphuis, 1993; Ding, Wang, & Jia, 2006; Droenen & Deigaard, 2007; Lesser, Roelvink, Kester, & Stelling, 2004; Roelvink & Banning, 1994; Roelvink, Walstra, & Chen, 1995; Zyserman & Johnson, 2002), which determine the sediment evolution using the both horizontal and vertical variations of the waves and currents.

The Opti-Morph model described in this paper is based on optimal control. In the past, the use of optimization theory has primarily been used in the design of coastal defense structures, whether in the design of ports and offshore breakwaters (Isebe, Azerad, Mohammadi, & Bouchette, 2008) or the protection of sandy beaches (Bouharguane, Azerad, Bouchette, Marche, & Mohammadi, 2010; Isèbe, Azerad, Bouchette, Ivorra, & Mohammadi, 2008). Optimal control can also be used in the modeling of shallow water morphodynamics, based on the assumption that the seabed acts as a flexible structure and adapts to a certain hydrodynamic quantity (Bouharguane et al., 2010; Mohammadi & Bouharguane, 2011). We will be continuing this study with the objective of producing a numerical morphodynamic model and validating it by comparing it to another well-established morphodynamic model.

## 1.2 Hypotheses

The Opti-Morph model is based on a certain number of assumptions. Given that the model is based on the minimization of a cost function, certain hypothesis must be made regarding the choice of this function. This function which originates from a physical quantity must be directly linked to the elevation of the seabed. At present, we set the quantity to be minimized as the energy of shoaling waves. This implies that the seabed reacts to the state of the waves by minimizing the energy of shoaling waves. Other assumptions assess the behavior of seabed and originate from general observations. Sediment transport is influenced by the orbital velocity of water particles (Soulsby, 1987), which leads to a greater sediment mobility in shallower waters. Another natural observation concerns the slope of the seabed, which cannot be overly steep without an avalanching process occurring (Reineck & Singh, 1973). Finally, in an experimental flume configuration, the quantity of sand must remain constant over time, with no inflow or outflow of sand to alter the sandstock.

## 2 Theoretical Developments

### 2.1 Modeling Framework

For the sake of simplicity, we present the principle in a one-dimensional setting. This enables us to compare the numerical results based on this theory with experimental flume data. No assumptions were made regarding the choice of dimension, and as a result it is relatively straightforward to extend this theory to a two-dimensional configuration.

We denote  $\Omega := [0, x_{\max}]$  the cross-shore profile of the active coastal zone, where  $x = 0$  indicates the location of the depth of closure, i.e. the location seaward of which there is no significant change in bottom elevation and  $x_{\max}$  is an arbitrary point at the shore, beyond the shoreline. The elevation of the seabed is a one dimensional positive

function, defined by:  $\psi : \Omega \times [0, T] \times \Psi$  where  $[0, T]$  is the duration of the simulation (s) and  $\Psi$  is the set of physical parameters describing the characteristics of the seabed. In order to model the evolution over time of  $\psi$  and given the assumption that the seabed  $\psi$  changes over time in response to the energy of shoaling waves, a description of the surface waves is needed.

## 2.2 Hydrodynamic Model

The morphodynamic model requires a description of the state of the water waves. Of course different models exist. We present the approach with a simple hydrodynamic model based on linear wave theory (Dean & Dalrymple, 2004) which is briefly described in Appendix A.

## 2.3 Morphodynamic Model by Wave Energy Minimization

The evolution of the seabed is assumed to be driven by the minimization of a cost function  $J$ . Given the hypotheses assumed in 1.2, the shape of the seabed is determined by the minimization of the potential energy of shoaling waves, for all  $t \in [0, T]$ :

$$J(\psi, t) = \frac{1}{16} \int_{\Omega_S} \rho_w g H^2(\psi, x, t) dx \quad [J.m^{-1}] \quad (1)$$

where  $\Omega_S$  is a time-dependent subset of  $\Omega$  over which the waves shoal and  $H$  denotes the height of the waves over the cross shore profile (see Appendix B),  $\rho_w$  is water density ( $kg.m^{-3}$ ) and  $g$  is the gravitational acceleration ( $m.s^{-2}$ ). In order to describe the evolution of the seabed, we assume that the seabed  $\psi$ , in its effort to minimize  $J$ , verifies the following dynamics:

$$\begin{cases} \psi_t = -\Upsilon \Lambda d \\ \psi(t=0) = \psi_0 \end{cases} \quad (2)$$

where  $\psi_t$  is the evolution of the seabed over time [ $m.s^{-1}$ ],  $\Upsilon$  is the abrasion of sand [ $m.s.kg^{-1}$ ] and  $\Lambda$  is the excitation of the seabed by the water waves.

The approach only involves two hyper-parameters with clear physical interpretation. The first hyper-parameter  $\Upsilon$  takes into account the physical characteristics of the sand and represents the mobility of the sediment. At the present time, we consider  $\Upsilon$  to be a measure of sand mobility expressed in  $m.s.kg^{-1}$ . Further explanation of the nature of this parameter will be given at a later stage of the models development. The second hyper-parameter  $\Lambda$  is a local function which represents the influence of the water depth on the seabed and is defined using an orbital velocity damping function (Soulsby, 1987):

$$\begin{aligned} \varphi : \Omega \times [0, h_0] &\longrightarrow \mathbb{R}^+ \\ (x, z) &\longmapsto \frac{\cosh(k(h - (h_0 - z)))}{\cosh(kh)} \end{aligned} \quad (3)$$

In unconstrained circumstances, for instance if a total sand volume constraint does not need to be enforced,  $d = \nabla_{\psi} J$ , which indicates a direction for local minimization of  $J$  with regards to  $\psi$ . However, constraints are added to the model to incorporate more physics and deliver more realistic results. Driving forces behind the morphological evolution of the seabed are described by the minimization of the cost function  $J$ . Secondary processes are expressed by constraints. In the interest of simplicity, we have adopted two physical constraints though more can be introduced if necessary. The first concerns the slope of the seabed. Depending on the composition

of the sediment, the slope of the seabed is bounded by a grain-dependent threshold  $M_{\text{slope}}$  (Dean & Dalrymple, 2004). This is conveyed by the following constraint:

$$\left| \frac{\partial \psi}{\partial x} \right| \leq M_{\text{slope}} \quad (4)$$

The dimensionless parameter  $M_{\text{slope}}$  represents the critical angle of repose of the sediment, and varies between 0.2 and 0.6 (Beakawi Al-Hashemi & Baghabra Al-Amoudi, 2018).

A second example concerns the sand stock in the case of an experimental flume. This constraint states that the quantity of sand in a flume must be constant over time, as given by (5), contrarily to an open-sea simulation where sand can be transported between the onshore and the offshore zones (Hattori & Kawamata, n.d.; Quick, 1991).

$$\int_{\Omega} \psi(t, x) dx = \int_{\Omega} \psi_0(x) dx \quad \forall t \in [0, T] \quad (5)$$

This constraint is necessary for verifying and validating the numerical model with physical simulations.

### 3 Numerical Application

This section is devoted to presenting the numerical results of the Opti-Morph model. In an effort to validate the model, the resulting seabed is compared to experimental flume data and the seabed produced by XBeach’s morphodynamic model. A brief description of the experiment is provided, as well the XBeach model.

#### 3.1 Description of the Experiment

The experimental observations presented here were collected as part of the COPTER project and a series of laboratory wave-flume experiments were performed in order to investigate the morphodynamic impact of introducing solid geotextile tubes to the Hatzuk (Israel) sea floor (Bouchette, 2017). We use the data collected without tubes to describe the natural evolution of the seabed over time.

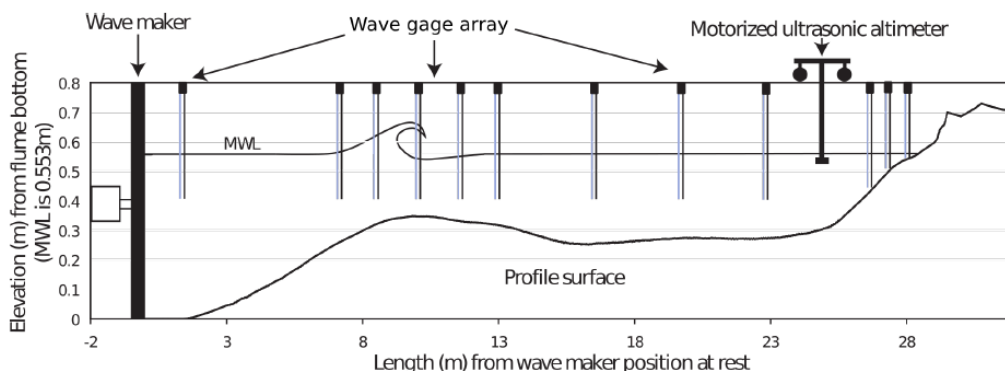


**Figure 1.** Diagram of the flume experiment.

A glass flume measuring 36m long, 0.55m wide and 1.3 meters deep is equipped with a wave maker and gauges measuring the height of the water. Artificial particles

are placed inside the flume representing the mobile sea bottom and an ultrasonic gauge is used to measure the sedimentary topography.

The experimental seabed, described in figure 1 is subjected to a 30 minute storm climate, representing fair weather conditions, with  $H_s = 135mm$  and  $T_s = 2.5s$ . Time and length scale ratio are set to 1/3 and 1/10 respectively to that of the field.

### 3.2 XBeach Model

As mentioned in the introduction, the XBeach model is an open source process-based model developed by Deltares, UNESCO-IHE and Delft University of Technology to simulate the hydro-morphodynamic processes in coastal areas.

In brief, XBeach uses four interconnected modules to model near shore processes (Daly, 2009). The two hydrodynamic modules consist of the short wave module and the flow module. The first is based on wave action equations (Holthuijsen, Booij, & Herbers, 1989), and incorporates breaking, dissipation (Roelvink, 1993) and wave current interactions, while the latter is governed by shallow water equations (Andrews & McIntyre, 1978; Walstra, Roelvink, & Groeneweg, 2000). One of the two morphodynamic modules is the sediment transport module based on the equilibrium sediment concentration equation (Soulsby, 1997) and a depth-averaged advection-diffusion equation (Galappatti & Vreugdenhil, 1985). The other is the morphology module which concerns seabed transformations such as the evolution of the seabed and avalanching.

In order to configure the XBeach model for the experimental flume setting, we refer to the XBeach user manual (Roelvink et al., 2010). The domain  $\Omega$  is defined over 30 meters with a uniform subdivision of 320 cells. The incoming wave boundary condition is provided using the JONSWAP wave spectrum (Hasselmann et al., 1973), with a significant wave height of  $H_{m0} = 0.015m$  and a peak frequency at  $f_p = 0.4s^{-1}$ . The breaker model uses the Roelvink formulation (Roelvink, 1993), with a breaker coefficient of  $\gamma = 0.4$ , a power  $n = 15$  and a wave dissipation coefficient of  $\alpha = 0.5$ . Concerning sediment parameters, the  $D50$  coefficient is set as  $0.0006$  and the porosity is  $2650kgm^{-3}$ . No other parameters such bed friction or vegetation were applied. The model is set to run for a period of 1800s.

### 3.3 Numerical Results

The Opti-Morph model was applied to the configuration of the COPTER experiment of section (3.1), and the resulting beach profile is shown by the red profile in figure 2. We observe a slight decrease ( $2cm$ ) of the height of the sandbar at  $x = 29m$  as well as the slope near the wave maker. The slope leading to the shore remains relatively unchanged.

A comparison was made between Opti-Morph (red), XBeach (blue) and the experimental data (green), as shown on figure 2. The red seabed profile provided by the Opti-Morph model shows a general quantitative agreement when compared to the experimental data, as does the XBeach morphological module. In fact, both models coincides with the experimental data over the plateau located at 15m-25m from the wave-maker (fig. 2B). At the shore, Opti-Morph matches the experimental data whereas XBeach shows a vertically difference of up to 3cm at  $x = 27m$  (fig. 2C). Discrepancies on the part of both models occur in the area surrounding the tip of the sandbar, as both Opti-Morph and XBeach fail to predict the advancing of the sandbar (fig. 2D); the experimental data show that the height of the bar remains at the same elevation before and after the time lapse, but has advanced towards the coast, an occurrence that neither numerical model was able to predict.

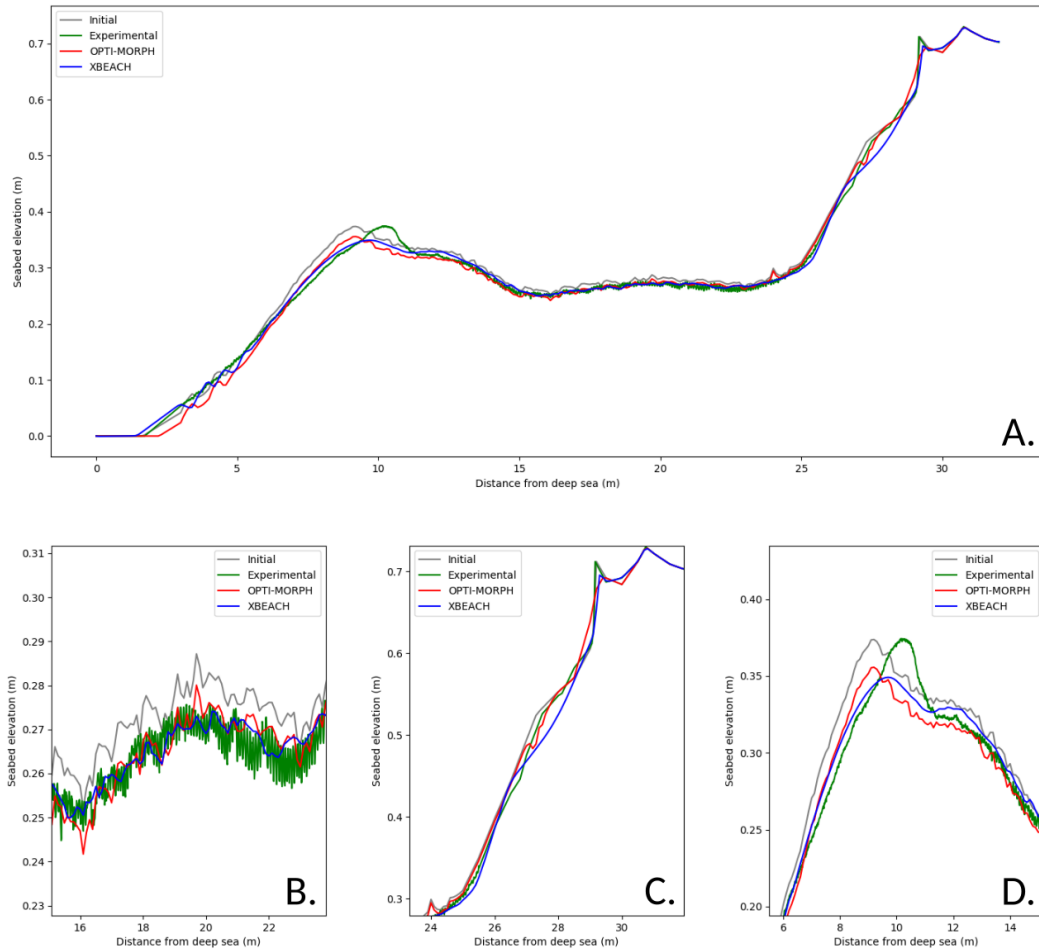


**Figure 2.** **A.** Results of the numerical simulation calculated over the initial seabed (black) using the XBeach morphodynamic module (blue) and the Opti-Morph model (green). These are compared with the experimental data acquired during the COPTER project (orange). **B.** Zoomed in view of the plateau section. **C.** Zoomed in view at the shoreline. **D.** Zoomed in view of the sandbar.

As such, this new model based on wave-energy minimization shows potential when compared to XBeach, in the case of a short term simulations.

## 4 Discussion

### 4.1 Long term simulation

This section is devoted to the long term behavior of Opti-Morph, the main question being, is this model capable of creating an equilibrium state after a great number of storm events regularly repeated.

The storm simulation of section 3.3 was repeated 10 times to create a long term time series. With Opti-Morph and XBeach set at the same configurations, this time series was applied to the same initial seabed. The resulting seabeds are shown in figure 3.



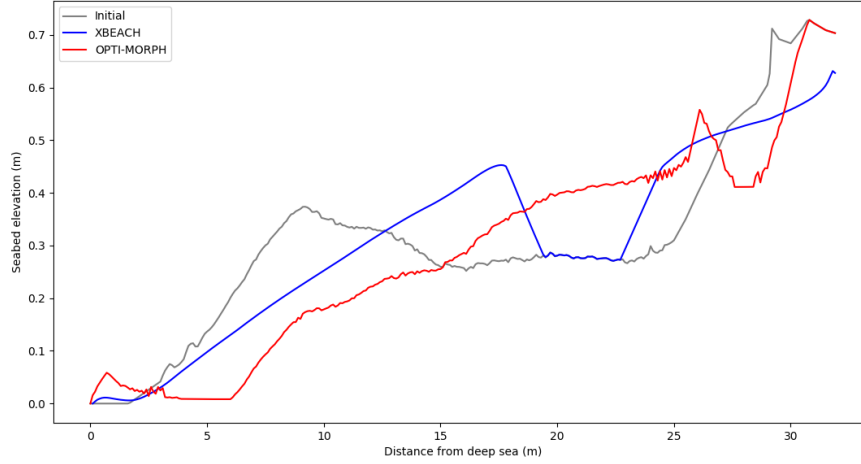


**Figure 3.** Comparison of seabeds produced by Opti-Morph and XBeach over a longer time series.

In the case of Opti-Morph, we observe the creation of a sandbar at 26m from the wave maker. A plausible assumption made from the short term simulations is that the initial sandbar situated at 9m, would continue to collapse when a longer time series is applied. This is however not the case. A sandbar, created independently from the initial bar can be observed at 26m as well as the creation of a trough (26 - 28m). This behavior is highly realistic as observed by [ref Copter 3D] and is an indicator of the seabed having reached a state of equilibrium.

XBeach however doesn't produce the same result, with a trough appearing at 20 - 23m, the depth of which has been stopped by the bedrock.

In the squash zone, we observe that the shape of the seabed is once again realistic. The slope at the 28-30m mark is noticeably steeper than that of the initial seabed. This is often observed in long-term storm profiles as shown by [ref]. In comparison, XBeach fails to produce this outcome, with a slope significantly less steep than the initial beach profile. After a series of storms, this outcome is impossible [ref].

To conclude the discussion of long-term simulations, Opti-Morph outperforms XBeach in this given configuration. The appearance of the sandbar and trough is typical behavior of the seabed after a series storm profiles, and the sharp incline of the seabed at the squash zone is another testimony of the potential of Opti-Morph. Comparing this model to XBeach, the qualitative behavior of Opti-Morph is better.

## 4.2 Parameter robustness analysis

One of the advantages of the Opti-Morph model is the low number of morphodynamic parameters required. At the present time, Opti-Morph requires two parameters: the mobility parameter  $\Upsilon$  and the maximal slope parameter  $M_{\text{slope}}$ . Here, an assessment on the robustness of the morphodynamic parameters is conducted.

Each simulation was run in the same configuration as the results of section 3.3, with the exception of the modification of the parameter in question. The results can be found in figure 4.

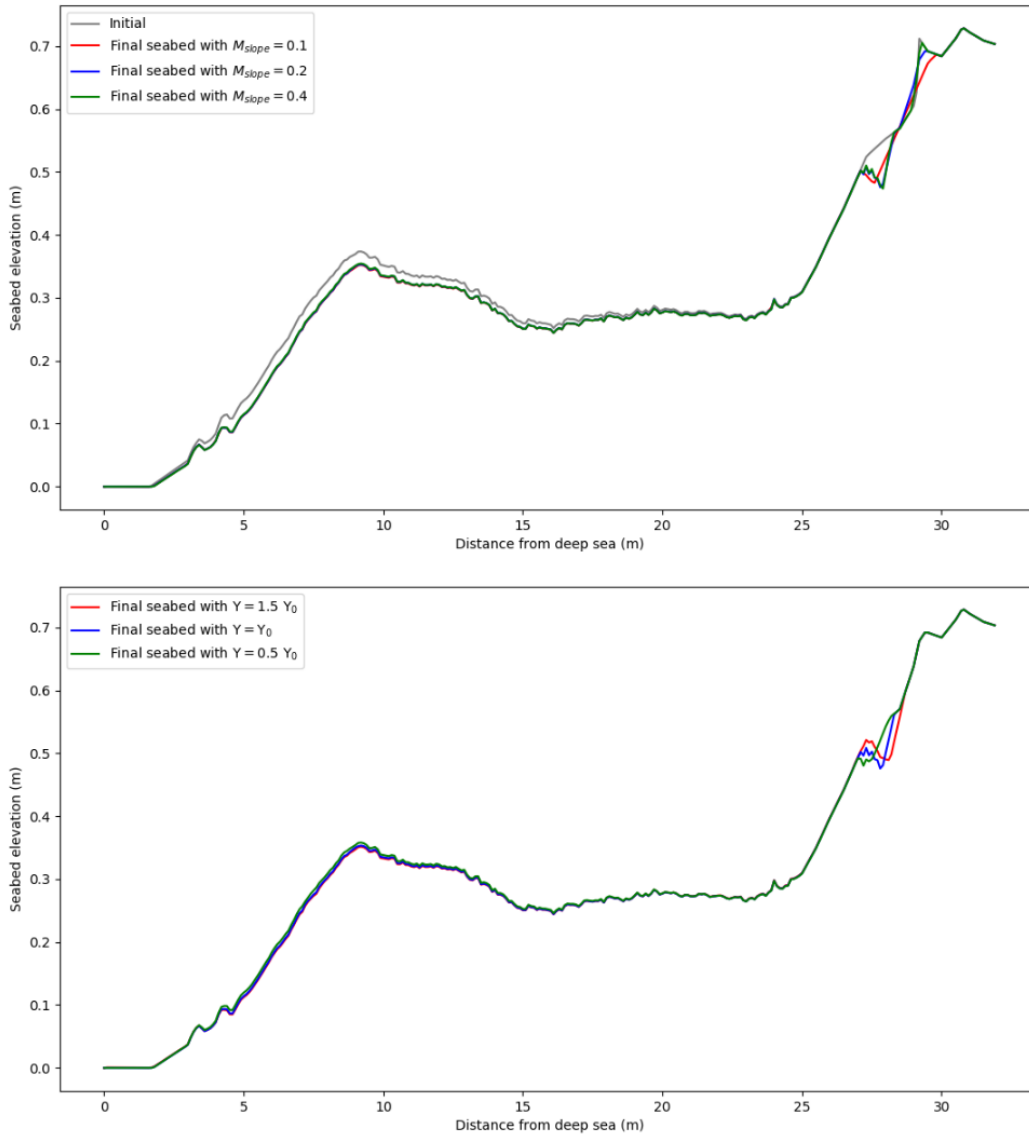


**Figure 4.** Top: Seabeds produced by Opti-Morph with different values of the maximal slope parameter  $M_{slope}$ . Bottom: Seabeds produced by Opti-Morph with different values of the mobility parameter  $\Upsilon$ .

In the study of the robustness of the slope parameter  $M_{slope}$ , illustrated in the top graph of figure 4, small discrepancies can be observed at the coast, where the slope is at its steepest. However, these discrepancies are deemed insignificant, which demonstrates the stability of Opti-Morph with regard to  $M_{slope}$ .

Similar observations can be made regarding the mobility parameter  $\Upsilon$ . Given the undisclosed nature of this parameter, beyond representing sediment mobility in  $m.s.kg^{-1}$ , this study was conducted in comparison to the value of  $\Upsilon$  used in 3.3 in the short-term simulations and denoted  $\Upsilon_0$ . The blue profile of the bottom graph of figure 4 depicts a seabed with  $\Upsilon = \Upsilon_0$ . The red profile depicts a seabed with a 50% increase in mobility, and the green profile a 50% decrease in mobility. All three profiles are close to identical over the entirety of the domain, with the exception of the coast line, where small discrepancies can be observed. The robustness of Opti-Morph in relation

to the mobility parameter  $\Upsilon$ , despite a significant increase or decrease of mobility, is apparent.

## 5 Conclusion

This model shows potential as a fast, robust and low complexity morphodynamic model involving only two hyper-parameters. Despite using a basic hydrodynamic model for the description of the complex coupling of the hydrodynamic and morphodynamic processes, we can nevertheless observe that the numerical simulation based on an optimization theory reproduces certain natural coastal mechanisms, such as the formation of sandbars and coastal erosion during severe weather conditions. These results demonstrate the tremendous potential of Opti-Morph, a constrained energy minimization morphodynamic model.

## Acknowledgments

The experimental observations presented here were collected as part of the COPTER project (LEGI, France) under the supervision of GLADYS ([www.gladys-littoral.org](http://www.gladys-littoral.org)) which has funded the project at the origin of the shore optimizer developed herein.

All data, models, and code generated or used during the study appear in the submitted article.

## A Hydrodynamic Model

In this section we present the hydrodynamic model based on the linear wave theory (Dean & Dalrymple, 2004). More sophisticated models can be applied as well as far as the model can be linearized for sensitivity analysis and that the corresponding numerical implementation has a significantly short run-time.

Given the current choice of cost function, a model capable of providing significant wave height is required. This model has the added advantage of expressing wave height as an explicit function of the seabed, which leads to rapid calculations of the morphodynamic model.

Let  $h$  be the depth of the water from a mean water level  $h_0$ . Ocean waves, here assumed monochromatic, are characterized by phase velocity  $C$ , group velocity  $C_g$  and wave number  $k$ , determined by the linear dispersion relation (A.1), where  $\sigma$  is the pulsation of the waves and  $g$  is the gravitational acceleration.

$$\sigma^2 = gk \tanh(kh) \tag{A.1}$$

We define  $\Omega_S$  as the time-dependent subset of  $\Omega$  over which the waves shoal and  $\Omega_B$  the subset of  $\Omega$  over which the waves break. Munk's breaking criterion (Munk, 1949) enables us to define  $\Omega_S(t) = \left\{ x \in \Omega, \frac{H(x,t)}{h(x,t)} < \gamma \right\}$  and  $\Omega_B(t) = \left\{ x \in \Omega, \frac{H(x,t)}{h(x,t)} \geq \gamma \right\}$ , where  $\gamma$  is a wave breaking index.

$$H(x,t) = H_0(t)K_S(x,t) \tag{A.2}$$

The height of the waves  $H$  over the cross shore profile is inspired by the shoaling equation (A.2), where  $H_0(t)$  is the deep water wave height and  $K_S$  is a shoaling coefficient, given by

$$K_S = \left( \frac{1}{2n} \frac{C_0}{C_g} \right)^{\frac{1}{2}} \quad (\text{A.3})$$

where  $C_0$  is the deep water wave velocity, and where

$$n = \frac{C}{C_g}, \quad C = C_0 \tanh(kh), \quad C_g = \frac{1}{2}C \left( 1 + \frac{2kh}{\sinh(kh)} \right). \quad (\text{A.4})$$

Instead of considering that waves depend solely on offshore wave height  $H_0$ , this model suggests that shoaling waves are decreasingly influenced by seawards waves. The greater the distance, the less effect it has of the present wave height. As such, we introduce a weighting function  $w$ . Assuming that the maximal distance of local spatial dependency of a wave is denoted  $d_w$ , the weighting function over the maximal distance  $d_w$  is given by  $w : [0, d_w] \mapsto \mathbb{R}^+$  such that  $w(0) = 1$ ,  $w(d_w) = 0$  and decreases exponentially.

Equation (A.2) for shoaling wave height becomes equation (A.5), where  $H_0^w$  is defined by (A.6).

$$H(x, t) = H_0^w(x, t)K_S(x, t) \quad (\text{A.5})$$

$$H_0^w(x, t) = \frac{1}{\int_{x-X}^x w(x-y)dy} \int_{x-X}^x w(x-y)H(y)K(y)dy \quad (\text{A.6})$$

Equation (A.5) applies only to the shoaling, nearshore-dependent waves of  $\Omega_S$ , significant wave height over the cross-shore profile  $H : \Omega \mapsto \mathbb{R}^+$  is defined by (A.7), where  $\alpha(x) = \frac{x}{d_w}$  over  $[0, d_w]$  to allow a smooth transition between offshore and nearshore-dependent waves.

$$H(x, t) = \begin{cases} [(1 - \alpha(x))H_0(t) + \alpha(x)H_0^w(x, t)] K_S(x, t) & \text{if } x \in \Omega_S \text{ and } x < d_w \\ H_0^w(x, t)K_S(x, t) & \text{if } x \in \Omega_S \text{ and } x \geq d_w \\ \gamma h(x, t) & \text{if } x \in \Omega_B \end{cases} \quad (\text{A.7})$$

### A.1 Numerical simulation

This section is devoted to the comparison of the hydrodynamic models with the data obtained in the experimental flume of section 3.1.

Figure A.1 depicts the three mean wave height profiles calculated over the storm simulation presented in section 3.1, where red represents the mean wave height produced by Opti-Morph, the blue is that of XBeach and the green points show the mean wave height calculated using the measures taken by the gauges of the flume.

Figure A.1 show that XBeach's hydrodynamic module (in blue) is significantly superior to that Opti-Morph's (in red), with a close qualitative fit with the experimental measurements excluding, as is often the case, the second point. ref ? Opti-Morph has an excessively dissipative impact on the mean wave height, with discrepancies of over 0.05m at the coast. An anti-dissipative effect can be assigned to the wave height in Opti-Morph's hydrodynamic module as a means to obtain a better quantitative fit with the experimental data. The resulting wave height (orange) is closer to the targeted experimental wave height.

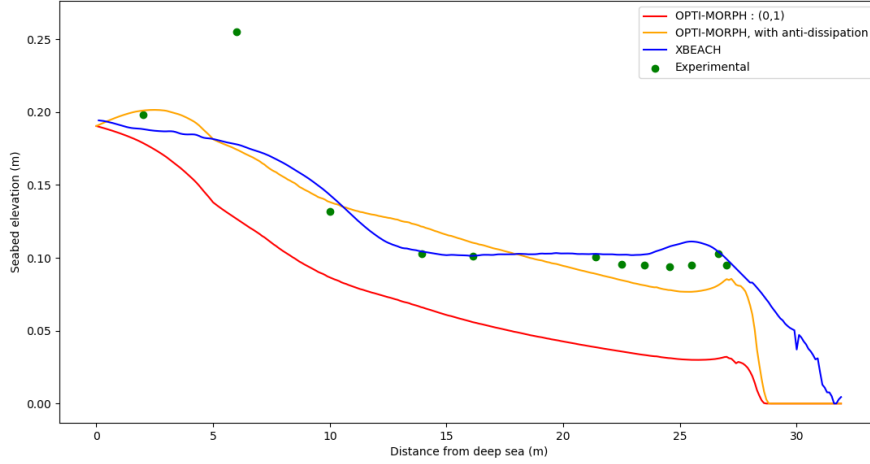


**Figure A.1.** Comparison of mean wave height over a storm simulation. The green points corresponds the the mean wave height provided by the gages of the flume experiment. The mean wave height determined by Opti-Morph (red) and XBeach (blue) also appear. Opti-Morph has the option to include an anti-dissipative effect to achieve a better fit with regards to the experimental data.

## B Gradient of the functional with respect to the bathymetry: $\nabla_{\psi} J$

Opti-Morph requires the evaluation of gradient of the functional  $J$  with respect to the bathymetry  $\psi : \nabla_{\psi} J$ . For a general functional of the form  $J(\psi(x), H(\psi(x)))$  involving dependencies with respect to the bathymetry and hydrodynamic quantities  $H$ , this sensitivity can be expressed using the chain rule:

$$\nabla_{\psi} J = \partial_{\psi} J + \partial_H J \partial_{\psi} H \quad (\text{B.1})$$

where  $H_{\psi}$  requires the linearization of the hydrodynamic model, and  $\psi$  is a parameteric representation of the bathymetry.

In situations where this linearization is impossible, for instance because the hydrodynamic model is a black-box, or too difficult, the gradient can be obtained using first-order finite difference approximations:

$$\nabla_{\psi} J|_i \approx \frac{J(\psi(x + \varepsilon e_i), H(\psi(x + \varepsilon e_i))) - J(\psi(x), H(\psi(x)))}{\varepsilon} \quad (\text{B.2})$$

where  $e_i(x_j) = \delta_{ij}$ . Typical relative value of  $\varepsilon$  is about three order of magnitude lower than the local water depth with a minimum value of  $10^{-4}$ . A second order approximation can be used as well doubling the cost of the evaluation. As the level of uncertainties is high is such a simulation, for instance, due to the estimation of sand abrasion coefficient for a given site. For the sake of simplicity, we have omitted the time dependency in the formulas.

### B.1 Gradient of the wave height with respect to the bathymetry: $\nabla_{\psi} H$

This section is devoted to the calcul of the gradient of the wave height  $H$ , given by (A.7), with regards to the seabed elevation  $\psi$ . Being as  $h = h_0 - \psi$ , the derivation of the third line of (A.7) with regards to  $\psi$  is immediate. The calcul of the gradient

of the first line of (A.7) is analogous to that of the second. It remains to differentiate the second line of (A.7) with regards to  $\psi$ . Observing that the chain rule yields for all  $x, t \in \Omega_S \times [0, T]$  with  $x \geq d_w$ ,

$$\nabla_\psi H(x, t) = H_0^w(x, t) \nabla_\psi K_S(x, t) + \nabla_\psi H_0^w(x, t) K_S(x, t), \quad (\text{B.3})$$

and that the term  $\nabla_\psi H_0^w(x, t)$  can be determined iteratively, using  $\nabla_\psi H_0 = 0$ , it remains to determine  $\nabla_\psi K_S(x, t)$ . Injecting the definitions of  $n$ ,  $C$  and  $C_g$ , given in (A.4), yields

$$K_S(x, t) = \left[ \tanh(kh) \left( 1 + \frac{2kh}{\sinh(kh)} \right) \right]^{1/2}. \quad (\text{B.4})$$

For the sake of simplicity, let  $U = \tanh(kh) \left( 1 + \frac{2kh}{\sinh(kh)} \right)$  and  $X = kh$ . Equation (B.4) becomes

$$\nabla_\psi K_S(x, t) = -\frac{1}{2} U^{-3/2} \nabla_\psi U, \quad (\text{B.5})$$

and we have

$$\nabla_\psi U = X_\psi \left[ \frac{1}{\cosh^2(X)} \left( 1 + \frac{2X}{\sinh(X)} \right) + 2 \tanh(X) \frac{\sinh(X) - X \cosh(X)}{\sinh^2(X)} \right], \quad (\text{B.6})$$

with  $X_\psi = k_\psi h + kh_\psi = k_\psi h - k$ . Moreover, differentiating both sides of the dispersion equation (A.1) by  $\psi$  gives

$$k_\psi = \frac{k^2}{\cosh(kh) \sinh(kh) + kh}. \quad (\text{B.7})$$

Combining (B.5),(B.6),(B.7), we obtain  $\nabla_\psi K_S$  and therefore  $\nabla_\psi H$ .

## References

- Andrews, D. G., & McIntyre, M. E. (1978). An exact theory of nonlinear waves on a lagrangian-mean flow. *Journal of Fluid Mechanics*, 89(4), 609646. doi: 10.1017/S0022112078002773
- Beakawi Al-Hashemi, H. M., & Baghabra Al-Amoudi, O. S. (2018). A review on the angle of repose of granular materials. *Powder Technology*, 330, 397-417. Retrieved from <https://www.sciencedirect.com/science/article/pii/S0032591018301153> doi: <https://doi.org/10.1016/j.powtec.2018.02.003>
- Bouchette, F. (2017, March). *Coastal defense strategy along hatzuk beach (northern tel aviv, israel). insights from the copter physical experimentation with moveable bed* (Dr Houle report No. 17-1). Dr Houle.
- Bouharguane, A., Azerad, P., Bouchette, F., Marche, F., & Mohammadi, B. (2010, 06). Low complexity shape optimization and a posteriori high fidelity validation. *Discrete and Continuous Dynamical Systems-series B - DISCRETE CONTIN DYN SYS-SER B*, 13. doi: 10.3934/dcdsb.2010.13.759
- Briand, M.-H., & Kamphuis, J. (1993, 07). Sediment transport in the surf zone: A quasi 3-d numerical model. *Coastal Engineering*, 20, 135-156. doi: 10.1016/0378-3839(93)90058-G
- Bugajny, N., Furmanczyk, K., Dudzinska-Nowak, J., & Papliska-Swerpel, B. (2013, 01). Modelling morphological changes of beach and dune induced by storm on the southern baltic coast using xbeach (case study: Dziwnow spit). *Journal of Coastal Research*, 1, 672-677. doi: 10.2112/SI65-114.1
- Coeffe, Y., & Pechon, P. (1982, 01). Modelling of sea-bed evolution under waves action. *Proc. 18th ICCE*, 1. doi: 10.9753/icce.v18.71
- Daly, C. (2009). Low frequency waves in the shoaling and nearshore zone a validation of xbeach. *Erasmus Mundus Master in Coastal and Marine Engineering and Management (CoMEM)*, Delft University of Technology.

- Dean, R., & Dalrymple, R. (2004, 03). Coastal processes with engineering applications. *Coastal Processes with Engineering Applications*, by Robert G. Dean and Robert A. Dalrymple, pp. 487. ISBN 0521602750. Cambridge, UK: Cambridge University Press, March 2004..
- de Vriend, H., Bakker, W., & Bilsse, D. (1994, 07). A morphological behaviour model for the outer delta of mixed-energy tidal inlets. *Coastal Engineering*, 23, 305-327. doi: 10.1016/0378-3839(94)90008-6
- Ding, Y., Wang, S., & Jia, Y. (2006, 11). Development and validation of a quasi-three-dimensional coastal area morphological model. *Journal of Waterway Port Coastal and Ocean Engineering*, 132, 462476. doi: 10.1061/(ASCE)0733-950X(2006)132:6(462)
- Droenen, N., & Deigaard, R. (2007, 03). Quasi-three-dimensional modelling of the morphology of longshore bars. *Coastal Engineering*, 54, 197215. doi: 10.1016/j.coastaleng.2006.08.011
- Fleming, C., & Hunt, J. (1977, 11). Application of sediment transport model. In (p. 1184-1202). doi: 10.1061/9780872620834.070
- Galappatti, G., & Vreugdenhil, C. (1985). A depth-integrated model for suspended sediment transport. *Journal of Hydraulic Research*, 23(4), 359-377.
- Gravens, M. (1997, 08). An approach to modeling inlet and beach evolution. In (p. 4477-4490). doi: 10.1061/9780784402429.348
- Hasselmann, K., Barnett, T., Bouws, E., Carlson, H., Cartwright, D., Enke, K., ... Walden, H. (1973, 01). Measurements of wind-wave growth and swell decay during the joint north sea wave project (jonswap). , 1-95.
- Hattori, M., & Kawamata, R. (n.d.). Onshore-offshore transport and beach profile change. In *Coastal engineering 1980* (p. 1175-1193). Retrieved from <https://ascelibrary.org/doi/abs/10.1061/9780872622647.072> doi: 10.1061/9780872622647.072
- Holthuijsen, L., Booij, N., & Herbers, T. (1989, 05). a prediction model for stationary , short crested waves in shallow water with ambient current. *Coastal Engineering*, 13, 23-54. doi: 10.1016/0378-3839(89)90031-8
- Isèbe, D., Azerad, P., Bouchette, F., Ivorra, B., & Mohammadi, B. (2008). Shape optimization of geotextile tubes for sandy beach protection. *International Journal for Numerical Methods in Engineering*, 74(8), 1262-1277. Retrieved from <https://hal.archives-ouvertes.fr/hal-00411912> doi: 10.1002/nme.2209
- Isebe, D., Azerad, P., Mohammadi, B., & Bouchette, F. (2008). Optimal shape design of defense structures for minimizing short wave impact. *Coastal Engineering*, 55(1), 35-46. Retrieved from <https://hal.archives-ouvertes.fr/hal-00411905> doi: 10.1016/j.coastaleng.2007.06.006
- Johnson, H., Brker, I., & Zyserman, J. (1995, 08). Identification of some relevant processes in coastal morphological modelling. In (p. 2871-2885). doi: 10.1061/9780784400890.208
- Kana, T., Hayter, E., & Work, P. (1999, 03). Mesoscale sediment transport at southeastern u.s. tidal inlets: conceptual model applicable to mixed energy settings. *Journal of Coastal Research*, 15, 303-313.
- Larson, M., & Kraus, N. (1989, 07). Sbeach: Numerical model for simulating storm-induced beach change. report 1. empirical foundation and model development. , 266.
- Larson, M., Kraus, N., & Byrnes, M. (1990, 05). Sbeach: Numerical model for simulating storm-induced beach change. report 2. numerical formulation and model tests. , 120.
- Latteux, B. (1980, 03). Harbour design including sedimentological problems using mainly numerical technics. In (p. 2213-2229). doi: 10.1061/9780872622647.133
- Lesser, G., Roelvink, D. J., Kester, J., & Stelling, G. (2004, 10). Development and

- validation of a three-dimensional morphological model. *Coastal Engineering*, 51, 883-915. doi: 10.1016/j.coastaleng.2004.07.014
- Maruyama, K., & Takagi, T. (1988, 01). A simulation system of near-shore sediment transport for the coupling of the sea-bottom topography, waves and currents. *Proc. IAHR Symp. Math. Mod. Sed. Transp. Coastal Zone*, 300-309.
- Mohammadi, B., & Bouchette, F. (2014, 01). Extreme scenarios for the evolution of a soft bed interacting with a fluid using the value at risk of the bed characteristics. *Computers and Fluids*, 89, 7887. doi: 10.1016/j.compfluid.2013.10.021
- Mohammadi, B., & Bouharguane, A. (2011, 01). Optimal dynamics of soft shapes in shallow waters. *Computers and Fluids*, 40, 291-298. doi: 10.1016/j.compfluid.2010.09.031
- Munk, W. (1949, 12). The solitary wave theory and its application to surf problems. *Annals of the New York Academy of Sciences*, 51, 376 - 424. doi: 10.1111/j.1749-6632.1949.tb27281.x
- Nairn, R., & Southgate, H. (1993, 02). Deterministic profile modelling of nearshore processes. part 2. sediment transport and beach profile development. *Coastal Engineering*, 19, 57-96. doi: 10.1016/0378-3839(93)90019-5
- Nicholson, J., Brker, I., Roelvink, D. J., Price, D., Tanguy, J.-M., & Moreno, L. (1997, 07). Intercomparison of coastal area morphodynamic models. *Coastal Engineering - COAST ENG*, 31, 97-123. doi: 10.1016/S0378-3839(96)00054-3
- Quick, M. (1991). Onshore-offshore sediment transport on beaches. *Coastal Engineering*, 15, 313-332.
- Reineck, H.-E., & Singh, I. B. (1973). *Depositional sedimentary environments; with reference to terrigenous clastics [by] h.-e. reineck [and] i. b. singh* [Book]. Springer-Verlag Berlin, New York.
- Roelvink, D. J. (1993, 02). Dissipation in random wave groups incident on a beach. *Coastal Engineering - COAST ENG*, 19, 127-150. doi: 10.1016/0378-3839(93)90021-Y
- Roelvink, D. J., & Banning, G. (1994, 01). Design and development of delft3d and application to coastal morphodynamics. , 451-456.
- Roelvink, D. J., Reniers, A., van Dongeren, A., Thiel de Vries, J., Lescinski, J., & McCall, R. (2010, 01). Xbeach model description and manual.
- Roelvink, D. J., Reniers, A., van Dongeren, A., Thiel de Vries, J., McCall, R., & Lescinski, J. (2009, 11). Modelling storm impacts on beaches, dunes and barrier islands. *Coastal Engineering*, 56, 1133-1152. doi: 10.1016/j.coastaleng.2009.08.006
- Roelvink, D. J., Walstra, D.-J., & Chen, Z. (1995, 08). Morphological modelling of keta lagoon case. In (p. 3223-3236). doi: 10.1061/9780784400890.233
- Ruessink, G., & Terwindt, J. (2000, 02). The behaviour of nearshore bars on the time scale of years: A conceptual model. *Marine Geology*, 163, 289-302. doi: 10.1016/S0025-3227(99)00094-8
- Soulsby, R. (1987, 11). Calculating bottom orbital velocity beneath waves. *Coastal Engineering - COAST ENG*, 11, 371-380. doi: 10.1016/0378-3839(87)90034-2
- Soulsby, R. (1997, 01). Dynamics of marine sand. , 272.
- Walstra, D.-J., Roelvink, D. J., & Groeneweg, J. (2000, 01). Calculation of wave-driven currents in a 3d mean flow model. In (Vol. 276). doi: 10.1061/40549(276)81
- Wang, H., Miao, G., & Lin, L.-H. (1993, 06). A timedependent nearshore morphological response model. In (p. 2513-2527). doi: 10.1061/9780872629332.192
- Watanabe, A., Maruyama, K., Shimizu, T., & Sakakiyama, T. (1986, 12). Numerical prediction model of three-dimensional beach deformation around a structure. *Coastal Engineering Journal*, 29, 179-194. doi: 10.1080/05785634.1986.11924437
- Williams, J., Esteves, L., & Rochford, L. (2015, 05). Modelling storm responses on a high-energy coastline with xbeach. *Modeling Earth Systems and Environment*,



1. doi: 10.1007/s40808-015-0003-8

Yamaguchi, M., & Nishioka, Y. (1985, 11). Numerical simulation on the change of bottom topography by the presence of coastal structures. In (p. 1732-1748). doi: 10.1061/9780872624382.118

Zimmermann, N., Trouw, K., Wang, L., Mathys, M., Delgado, R., & Verwaest, T. (2012, 12). Longshore transport and sedimentation in a navigation channel at blankenberge (belgium). *Coastal Engineering Proceedings, 1*. doi: 10.9753/icce.v33.sediment.111

Zyserman, J., & Johnson, H. (2002, 05). Modelling morphological processes in the vicinity of shore-parallel breakwaters. *Coastal Engineering, 45*, 261284. doi: 10.1016/S0378-3839(02)00037-6